

A first-principles study on the adhesion of Pt layers to NiO(100) and IrO₂(110) surfaces

Jianhui Yang, Baihai Li, Jinzhi Wang, Liang Chen and Runwei Li

Institute of Materials Technology and Engineering, Chinese Academy of Sciences, Ningbo, Zhejiang 315201, People's Republic of China

E-mail: chenliang@nimte.ac.cn

Received 1 October 2009, in final form 10 November 2009

Published 3 December 2009

Online at stacks.iop.org/JPhysCM/22/015003

Abstract

We report a comparative study on the Pt/NiO and Pt/IrO₂ interfaces from first principles. It is found that Pt layers can bind with the IrO₂ surface much stronger than the NiO surface. The adhesion strength of Pt/NiO interfaces is dominated by the Pt–O ionic bond. The Pt layers induce corrugation of the oxide surfaces and loosen the Ni–O bonding strength. The dissolution of Ni atoms into the Pt slab appears to enhance the adhesion strength by forming stronger Ni–O bonds. In contrast, the adhesion strength of Pt/IrO₂ interfaces has contributions from both Pt–O ionic and Pt–Ir metallic bonds. Furthermore, the interfacial adhesion of IrO₂/NiO is also stronger than that of Pt/NiO interfaces. IrO₂ may work as glue layers to stabilize Pt/NiO films.

(Some figures in this article are in colour only in the electronic version)

1. Introduction

Pt/NiO films have been of intensive interest for applications in the resistance random access memory since the NiO crystalline thin film has an extraordinary repetitive resistance switching (RS) property [1–7]. However, the I – V curves of Pt/NiO films are not stable enough for memory switching, which makes Pt/NiO films encounter difficulties in practical device applications. The Pt–oxide interfacial reaction has a strong impact on the RS process [5]. Recently, Kim *et al* reported that the stability of the I – V curves can be significantly improved by inserting thin IrO₂ layers into the Pt/NiO interface [6]. The thin IrO₂ layer is able to greatly enhance the crystallinity of the interface (particularly the NiO phase).

Many experimental studies have been conducted to explore some Pt/NiO interfacial properties such as adhesion energy of the interface, elemental distributions and epitaxial orientations at the interface [8–12]. For example, Shieu used the electron microscopy and electron diffraction techniques to characterize the Pt/NiO interface that was prepared by epitaxial growth of polycrystalline platinum on the NiO(001) surface. They reported that the most favorable orientations between Pt and NiO are Pt(001)/NiO(001) and Pt(110)/NiO(110) [12]. Venkataraman employed a continuous microscratch technique to characterize the adhesion of as-sputtered Pt thin films to

NiO single crystals and found that the true adhesion energy for the as-sputtered Pt/NiO and the Pt/NiO annealed at 800 °C in air are 0.035 and 0.34 J m^{−2}, respectively, which include the influence of crystal defects [9, 11]. Interestingly, most of these experimental studies also show that there is a PtNi alloy phase between Pt and NiO due to Ni dissolution [8–11].

Despite the above experimental studies dealing with Pt/NiO interfaces, there is limited systematic study of the Pt/IrO₂ interface. Indeed, an atomistic understanding of the nature of the bonding of Pt layers to NiO and IrO₂ surfaces is a key step towards elucidating the different behaviors between Pt/NiO and Pt/IrO₂/NiO films. In this regard, we performed density functional theory (DFT) calculations to comparatively examine the Pt/NiO and Pt/IrO₂ interfaces. Our goal is to identify the most stable interfaces and compare the stability of these interfaces in terms of adhesion energy and electronic structures.

2. Computational methods

Spin-polarized DFT computations were performed using the Vienna *ab initio* simulation package (VASP) [13, 14], with projector augmented wave (PAW) pseudopotentials [15]. We used the generalized gradient approximation (GGA) with the

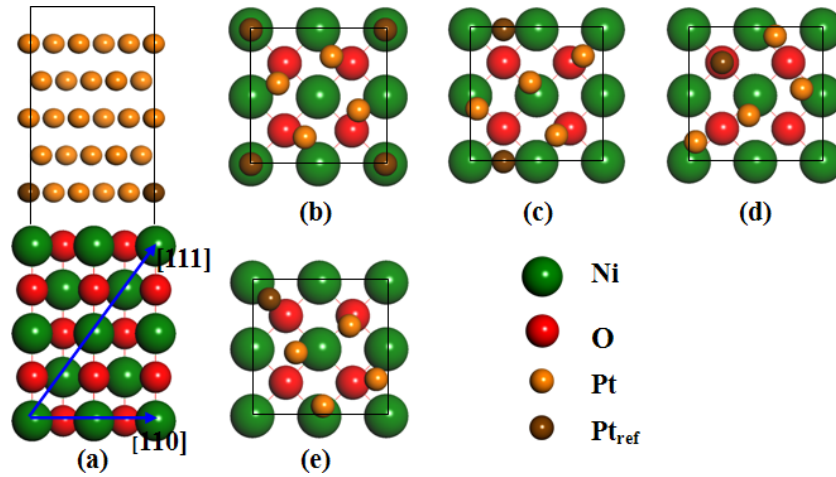


Figure 1. (a) Side view of the supercell: top view of the 5Pt(001)/4NiO(001) interface with P_{ref} (b) on the surface Ni atoms, (c) above the hollow site, (d) on the surface O atoms and (e) above the Ni–O bridge.

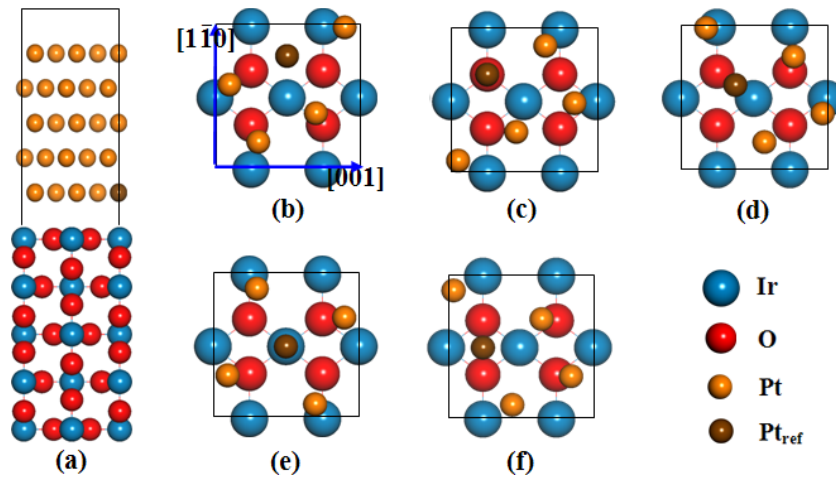


Figure 2. (a) Side view of the supercell: top view of the 5Pt(001)/4IrO₂(010) interface with P_{ref} (b) on the hollow site, (c) on the surface O atoms, (d) above the Ir–O bridge, (e) on the surface Ir atoms and (f) above the O–O bridge.

PW91 functional for the exchange–correlation energy. The GGA + U approach with the parameters $U = 6.3$ eV and $J = 1$ eV, which is able to provide an accurate description for metal oxides such as NiO [16–19], was chosen for Ni 3d electrons. Indeed, the magnetic moment of NiO using the parameters above was calculated to be $1.79 \mu_{\text{B}}$, which is in line with the experimentally observed values (1.64 – $1.9 \mu_{\text{B}}$) and other theoretical results (1.7 – $1.8 \mu_{\text{B}}$) [20, 21]. The structural optimizations were performed until the forces on each atom were less than $0.05 \text{ eV } \text{\AA}^{-1}$. The kinetic energy cutoff was set to 400 eV. The Brillouin zone was sampled within $5 \times 5 \times 1$ and $4 \times 4 \times 1$ Monkhorst–Pack meshes for the Pt/NiO and Pt/IrO₂ interfaces, respectively.

The lattice constant of the NiO bulk is calculated to be 4.18 \AA . IrO₂ has a rutile structure, with the calculated lattice parameters $a = b = 4.49 \text{ \AA}$, $c = 3.20 \text{ \AA}$ and $u = 0.31$. Pt has an FCC structure with a lattice parameter of 3.92 \AA . All these results are in good agreement with the experimental and previous theoretical results [20, 21]. In the present study, we chose five Pt(001), NiO(001) and IrO₂(110) layers to build

the $[5 + 5]$ Pt/NiO and $[5 + 5]$ Pt/IrO₂ supercells. The direct deposition of Pt layers onto the NiO or IrO₂ surfaces would lead to a large lattice mismatch of 6.2% and 11.9%, respectively. Such interfaces will be denoted as 4Pt/4NiO and 4Pt/4IrO₂ below since the (2×2) supercell contains four Pt atoms and four NiO (or IrO₂) units in each layer. To alleviate the large mismatch, we also constructed the interfaces by rotating and translating the Pt slab parallel to the oxide plane, with one reference Pt atom (P_{ref}) on each possible high-symmetry site. Such a strategy is inspired by the previous successful studies on Co/TiC interfaces [22]. It is therefore found that the 5Pt/4NiO (figure 1) and 5Pt/4IrO₂ interfaces (figure 2), with five Pt atoms on the (2×2) oxide surface in the supercell, can minimize the average lattice mismatch to 4.9% and 1.4%, respectively. Note that the lattice parameters of the oxide were kept fixed, while the Pt in-plane lattice parameter was adjusted accordingly in all calculations. The initial lengths of the Pt/NiO and Pt/IrO₂ supercells (perpendicular to the interface) were 22.95 and 26.95 \AA , respectively. Upon relaxation, the lengths are reduced by 1.10 and 1.40 \AA on

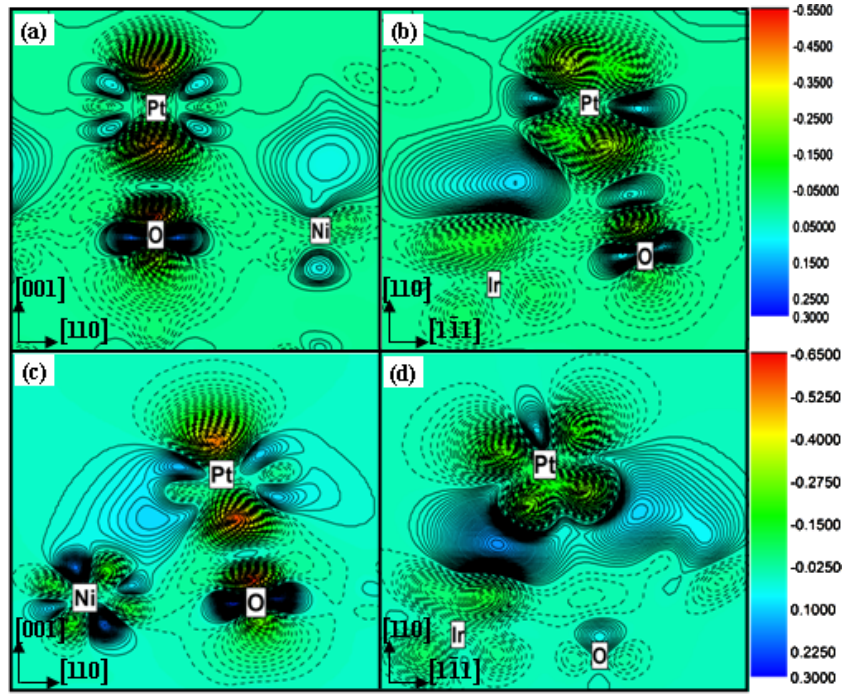


Figure 3. Calculated charge density differences for (a) the 5Pt(001)/4NiO(001) interface, (b) the 5Pt(001)/4IrO₂(010) interface, (c) a Pt monolayer on the NiO(001) surface and (d) a Pt monolayer on the IrO₂(010) surface.

average for Pt/NiO and Pt/IrO₂, respectively, which is mainly due to the contraction of the Pt interlayer distances.

3. Results and discussions

3.1. Pt(001)/NiO(001) interfaces

The adhesion strength of an interface can be evaluated by the ideal energy of adhesion $E_{ad} = (E_{s1} + E_{s2} - E_{interface})/2A$, where $E_{interface}$ is the total energy of the interface, E_{s1} and E_{s2} are the total energies of the individual slab in the same supercell of the corresponding interfaces and A is the interface area. The factor 2 in the denominator arises from the two identical interfaces per supercell. The calculated E_{ad} , the average interlayer distance between Pt and Ni (d_{Pt-Ni}) or O (d_{Pt-O}) and the minimum Pt–O bond lengths ($d_{min(Pt-O)}$) of the 5Pt/4NiO and 4Pt/4NiO interfaces are summarized in table 1. As expected, the 5Pt/4NiO interfaces generally exhibit higher E_{ad} than 4Pt/4NiO interfaces. The 5Pt/4NiO interface with Pt_{ref} right above the O atoms (O-top structure) is found to be energetically the most favorable with an E_{ad} of 0.70 J m⁻², while the Ni-top structure is the most unfavorable for both 5Pt/4NiO and 4Pt/4NiO interfaces. The average d_{Pt-O} perpendicular to the surface is slightly longer than d_{Pt-Ni} in all cases, indicating a corrugation at the interface. Ni atoms are relaxed slightly toward the Pt slabs, while surface O atoms, except the one in direct contact with Pt_{ref}, are relaxed toward the NiO phase. Another notable change to the surface structure is that the bond lengths between surface O atoms and their nearest Ni atom are slightly elongated from 2.09 to 2.2 Å. This is because the adhesion of Pt layers loosens the Ni–O

Table 1. Calculated adhesion energies (J m⁻²), interlayer distances and minimum Pt–O bond lengths (Å) of the Pt/NiO and Pt/IrO₂ interfaces. The values for the 4Pt/4NiO and 4Pt/4IrO₂ interfaces are shown in parentheses.

Pt/NiO interfaces	W_{ad}	d_{Pt-O}	d_{Pt-Ni}	$d_{min(Pt-O)}$
(b) Ni-top	0.63(0.45)	2.50(2.76)	2.44(2.70)	2.62(3.43)
(c) Hollow	0.69(0.56)	2.48(2.57)	2.43(2.49)	2.29(2.93)
(d) O-top	0.70(0.66)	2.56(2.43)	2.49(2.33)	2.14(2.43)
(e) Ni–O bridge	0.69(0.68)	2.53(2.45)	2.47(2.36)	2.19(2.52)
Pt/IrO ₂ interfaces	W_{ad}	d_{Pt-O}	d_{Pt-Ir}	$d_{min(Pt-O)}$
(b) Hollow	2.40(2.44)	2.37(2.26)	2.29(1.93)	2.17(2.83)
(c) O-top	2.39(2.16)	2.35(2.40)	2.27(2.37)	2.24(2.19)
(d) Ir–O bridge	2.39(2.91)	2.37(2.35)	2.30(2.31)	2.18(3.23)
(e) Ir-top	2.29(2.84)	2.53(2.38)	2.47(2.33)	2.70(3.23)
(f) O–O bridge	2.29(2.16)	2.38(2.50)	2.27(2.44)	2.46(2.74)

ionic bonds. Electrons flow from Pt atoms to the O ions and eventually arrive at the Ni ions.

In general, the minimum Pt–O bond length decreases when E_{ad} increases. It implies that the interactions between Pt and O atoms play a critical role in the Pt(001)/NiO(001) interfacial bonding. To further analyze the interfacial bonding, we examined the charge redistribution of the most stable 5Pt(001)/4NiO(001) interface with Pt_{ref} above the surface O atom. The charge density difference (figure 3(a)) reveals the formation of a strong Pt–O ionic bond, as confirmed by the 0.2e Bader charge transfer from Pt_{ref} to the surface O atom [23, 24]. At the same time, slight orbital hybridization occurs between Pt and the surface Ni atoms. This can be regarded as weak bonds with mixed metallic and covalent character [25]. In figure 4(a), we show the projected density

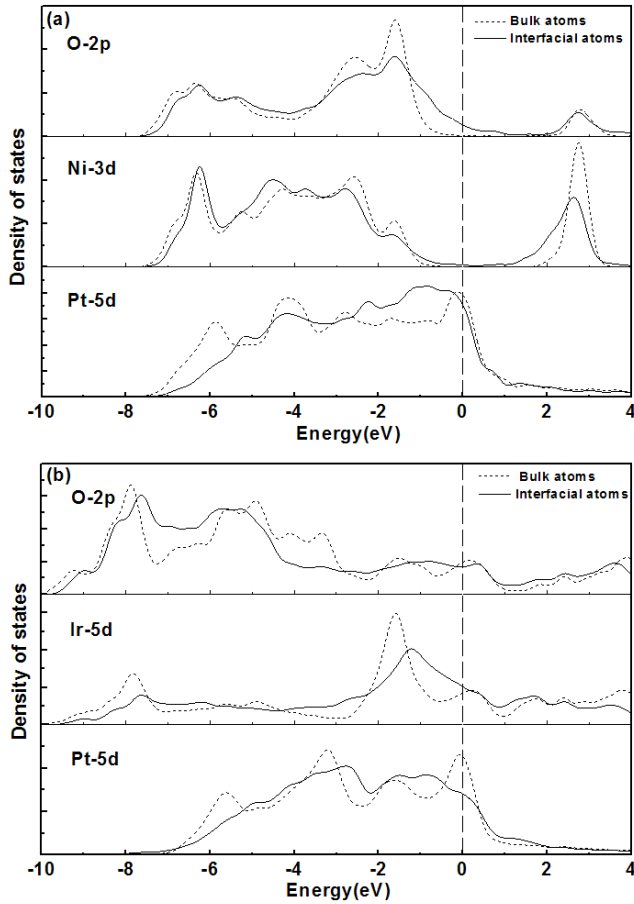


Figure 4. Calculated density of states of (top) the Pt/NiO interface with Pt_{ref} on the O-top site and (bottom) the Pt/IrO₂ interface with Pt_{ref} on the hollow site.

of states (PDOS) of the same interface. The solid lines represent the PDOS of the surface ions, which participate in the interfacial bonding. For comparison, the dashed lines represent the PDOS of the bulk ions that are far away from the interface. NiO exhibits a typical semiconductor character with a wide bandgap of around 3.0 eV. There is no remarkable difference between the PDOS of the ‘bulk’ and surface Ni ions, meaning that the surface Ni ions play a minor role in the interfacial binding with the Pt layer. Recall that only slight hybridization between Pt and Ni orbitals is observed in figure 3(a), namely Pt–Ni bonding has a more covalent rather than metallic character. This is mainly due to the relatively localized nature of Ni 3d electrons. In contrast, the O ions are more active and thus form an ionic bond with the surface Pt atom. Some density of states for surface O atoms at the Fermi level appears upon interacting with Pt layers, indicating the presence of some metallic character in the interface.

The overall adhesion strength is the summation of the binding strength at each site. In order to carefully evaluate the contribution from binding strength at an individual site, we also considered the case that one Pt monolayer is deposited on the NiO(001) surface. Here the monolayer means that all the identical high-symmetry sites (e.g. four Ni-top sites) on the (2 × 2) NiO surface are occupied. As expected, the O-

top site is identified as the only stable binding site. Note that the Pt–O bond length (1.98 Å) here is much shorter than the Pt(001)/NiO(001) interlayer distance. Consequently, the Pt monolayer can bind more strongly on the NiO(001) surface with an adhesion energy of 2.13 J m⁻². Each Pt atom donates around 0.12e to the substrate and formed ionic bonds with O atoms. In contrast, the direct deposition of the Pt atom above Ni atoms appears to be unstable upon energy minimization. Indeed, the strong positive Ni ions fail to interact with Pt atoms effectively. They are not able to firmly anchor Pt atoms because of the strong attractive O atoms nearby. The vast difference in the energetics would force Pt atoms to converge onto the O-top site immediately. Nevertheless, the interaction between Pt atoms and surface Ni atoms here appears to be stronger than at the Pt(001)/NiO(001) interfaces, as illustrated by the more pronounced electron hybridization between Pt 5d and Ni 3d orbitals (figure 3(c)). Correspondingly, the Pt–O bond is tilted by 12° from the surface normal, whereas the adhesion of Pt layers is still mainly determined by the Pt–O bonding.

Asides from E_{ad} , the stability of the interface is also influenced by the tensile strain of the Pt adlayers due to the lattice mismatch. Herein we evaluated the strain effect using $E_{\text{strain}} = E_{\text{Pt}}^{\text{A}} - E_{\text{Pt}}^{\text{O}}$, where E_{Pt}^{A} and E_{Pt}^{O} are the energies of Pt slabs with adjusted and original lattice parameters. The strain energies of 4Pt/4NiO and 5Pt/4NiO interfaces are calculated to be 0.05 and 0.02 eV per Pt atom, respectively. It is not surprising to see such moderate and similar values since the average lattice mismatch of the 4Pt/4NiO and 5Pt/NiO are actually close (6.2% and 4.9%). Therefore, the strain induced by the mismatch does not destabilize the Pt/NiO interfaces.

It was observed experimentally that a PtNi alloy phase exists at the Pt/NiO interface due to the dissolution of Ni atoms from NiO into Pt layers [10, 11]. In light of the previous report that Ni atoms are randomly distributed in the NiPt alloy [26], we next investigated the deposition of PtNi layers with varying compositions on the NiO(001) surface. As a preliminary step, we found that the slab containing five $\text{Pt}_{0.8}\text{Ni}_{0.2}$ units can yield a lattice parameter of 6.07 Å, which has a relatively small mismatch (2.97%) with the NiO(001) substrate. Thus, we built the 5($\text{Pt}_{0.8}\text{Ni}_{0.2}$)/4NiO(001) interfaces by the following scheme: (1) replace one Pt atom with the Ni atom per layer; (2) translate the 4Pt1Ni slab parallel to the NiO(001) plane to locate the Ni atom of the first layer at each high-symmetry site; (3) vary the Ni atom’s location at the second layer and (4) modify the fourth and fifth layers symmetrically in accordance with the first two layers. Certainly, there are plenty of variations of the interfacial structures. For simplicity, we only presented the average interlayer distance, the minimum Pt–O and Ni_{PtNi}–O bond lengths, and E_{ad} of the selected stable interfaces in table 2. The location of Ni atoms at the external layer appears to drastically influence E_{ad} , whereas E_{ad} is only slightly changed (within 0.02 eV) with different locations of Ni atoms at the second layer. The O-top structure yields an adhesion strength 10% higher than all 5Pt/4NiO interfaces, where the external Ni atom forms a short bond (~1.9 Å) with the surface O atoms. Indeed, Ni exhibits higher electropositivity than Pt so that it can form stronger Ni–O ionic bonds and enhance the interfacial bonding of NiPt/NiO.

Table 2. Calculated adhesion energies (J m^{-2}), interlayer distances and minimum Pt–O and Ni–O bond lengths (\AA) of the 4Pt1Ni/4NiO interfaces.

Interfaces	W_{ad}	$d_{\text{Pt-O}}$	$d_{\text{Pt-Ni}}$	$d_{\text{min(Pt-O)}}$	$d_{\text{min(Ni-O)}}$
Ni-top	0.65	2.49	2.42	2.29	3.28
Hollow	0.65	2.50	2.45	2.33	3.09
O-top	0.77	2.50	2.43	2.94	1.93
Bridge	0.64	2.54	2.48	2.23	2.91

Furthermore, Ni also donates electrons ($\sim 0.3e$) to Pt in the NiPt layers, leading to the formation of slightly positive Ni_{PtNi} ions. As a result, the E_{ad} of other 4Pt1Ni/4NiO(001) interfaces are even lower than those of 5Pt/4NiO interfaces due to the electrostatic repulsive interaction between the Ni_{PtNi} (in the PtNi phase) and surface Ni_{NiO} (in NiO) atoms.

3.2. Pt(001)/IrO₂(110) interfaces

For the Pt(001)/IrO₂(110) interfaces, it is unexpected that the un-rotated Pt slab with Pt_{ref} on the bridge site yields the highest E_{ad} of 3.57 J m^{-2} . However, the in-plane lattice parameter of the Pt slab has to be elongated by 12% to match the IrO₂ substrate. The strain energy of Pt layers is calculated to be 0.23 eV/atom , indicating that such a 4Pt/4IrO₂ interface is unrealistic. Instead, the average lattice mismatch of the rotated 5Pt/4IrO₂ interfaces (figure 2) is significantly reduced to 1.4%, thus yielding a slight strain energy of 0.02 eV/atom . At the 5Pt/4IrO₂ interfaces, the average interlayer distances are generally $0.15\text{--}0.2 \text{ \AA}$ shorter than those at the 5Pt/4NiO interfaces. Consequently, Pt layers can bind with IrO₂ much stronger than NiO, with E_{ad} ranging from 2.29 to 2.40 J m^{-2} (see table 1). In fact, the interfaces (b)–(d) in figure 2 share very similar configurations because of high symmetry. Roughly speaking, each interface contains one Pt on the hollow site, two Pt on the Ir–O bridge site, one Pt on the Ir-top site and one Pt on the O-top site. Therefore, the adhesion strengths of these interfaces are virtually identical ($\sim 2.39 \text{ J m}^{-2}$). Figure 3(b) displays the charge density difference of the interface (b) with Pt_{ref} residing on the bridge site. The Pt_{ref} atom forms a strong Pt–O ionic bond, as the associated O atom is dragged out of its original position. However, the bonding behavior is quite different from that of Pt/NiO interfaces. The Pt_{ref} atom is actually lying down on the IrO₂ surface, accompanied by the tilted O 2p orbital from the surface normal. At the same time, Pt_{ref} also binds with the nearest Ir atom strongly, as indicated by the pronounced electron accumulation between Pt and Ir atoms. Unlike the Pt–Ni bonding, very limited hybridization of Pt d and Ir d orbitals/states is observed here, while electrons are virtually delocalized at the interface. This reflects the nature of strong metallic bonding as well as very slight covalency. As shown in the PDOS (figure 4(b)), IrO₂ exhibits a remarkable metallic character. A significant change to the 5d states of the interfacial Ir atoms (particularly near the Fermi level) can be observed, indicating that Ir atoms play a very important role in the interfacial bonding. Indeed, a significant density of states near the Fermi level also demonstrates the strong metallic character

of the interfacial bonding. In addition, the O 2p states also participate in the bonding.

If we place one Pt monolayer on the IrO₂(110) surface, the hollow site turns out to be the most favorable binding site. The interaction between Pt and O, with a long bond distance of 2.83 \AA , does not single-handedly determine the adhesion strength. The two lobes of Pt d orbitals can form bonds with the two nearest Ir atoms simultaneously. Electrons are virtually depleted near the nucleus of Ir and Pt atoms, while nearly delocalized in the region between them (see figure 3(d)). As a result, the adhesion energy is further enhanced to 3.92 J m^{-2} . The monolayer can also be stably deposited on the O-top, Ir-top and Ir–O bridge sites, with E_{ad} of 3.28 , 2.55 and 2.68 J m^{-2} , respectively. With this information in mind, we now turn back to the Pt/IrO₂ interfacial structures. The interface (c) in figure 2 contains three Pt on the Ir-top sites and two Pt on the O-top sites. The interface (f) has one Pt on the O–O bridge site, two Pt on the hollow sites and two Pt on the O-top site. Although these two interfaces are quite different from the other three interfaces discussed above, they do not show significantly weaker adhesion strength (only 0.1 J m^{-2} lower in terms of E_{ad}). Indeed, the overall adhesion strength is the summation of the binding strength of each Pt atom with the oxide surface. Unlike the NiO surface, the O-top site is no longer the unique favorable binding site for Pt atoms. The IrO₂ surface can provide multiple binding sites in addition to strongly anchor Pt layers. As a result, the adhesion strength of Pt/IrO₂ interfaces is much stronger than that of Pt/NiO interfaces.

We are now in a position to interpret the different bonding behaviors for Ni–Pt and Ir–Pt by analyzing the electronic structures. It is known that Ni has higher electropositivity than Ir because of electron configurations ($3d^8 4s^2$ versus $5d^7 6s^2$). Hence, the neutral Ni atom can interact with Pt atoms more strongly than Ir atoms (1.83 eV versus 1.15 eV). The abundance of the Ni 4s electron reservoir enables Ni atoms to form strong metallic bonds with Pt atoms. Similarly, NiO has higher ionic character than IrO₂ because the two Ni 4s electrons would be more readily transferred to the O ions. However, the remaining Ni 3d electrons are quite localized so that the surface Ni ions can only form weak covalent bonds with Pt adatoms instead of strong metallic bonding due to the depletion of ‘hot’ Ni 4s electrons. Namely, Ni^{2+} ions exhibit lower electropositivity and reactivity than Ir^{2+} ions. They are relatively inert towards bonding with Pt layers. The interfacial bonding is thus dominated by the Pt–O ionic bonds. On the other hand, although the two Ir 6s electrons also flow to O ions in IrO₂, the remaining Ir 5d electrons are much more delocalized and active than the ‘frozen’ Ni 3d electrons. In other words, the ‘hot’ Ir 5d electrons are still able to participate in the bonding with Pt atoms by forming strong metallic bonds. These distinct behaviors of Ir 5d and Ni 3d electrons are clearly reflected in figure 3.

3.3. NiO(001)/IrO₂(110) interface

Finally, we examined the adhesion of NiO(001)/IrO₂(110) interfaces to further assess the validity of IrO₂ as glue layers. In order to mimic the deposition of NiO onto IrO₂

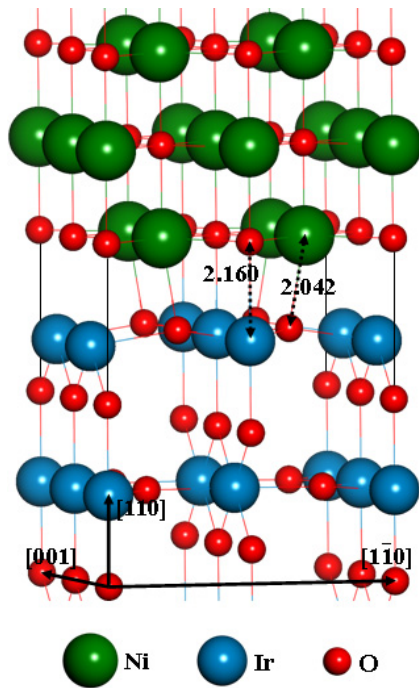


Figure 5. Side view of the NiO(001)/IrO₂(010) interface.

in experiments [6], we built a [5 + 5] NiO(001)/IrO₂(010) interface by keeping the lattice parameters of IrO₂ fixed at its bulk value and adjusting NiO adlayers accordingly. The average lattice mismatch is around 6.1%. Because of the strong ionic character of NiO and IrO₂, the greatest adhesion strength can be achieved when the Ir ions are placed above O_{IrO₂} (in IrO₂) so that the Ni ions can interact with O_{NiO} (in NiO) effectively in return (see figure 5). A very slight charge transfer ($\sim 0.06e$) from NiO to IrO₂ occurs. The interfacial Ni–O_{IrO₂} and Ir–O_{NiO} bond lengths are calculated to be 2.04 and 2.16 Å, respectively. In fact, the Ni–O_{IrO₂} bonds are slightly distorted and tilted from the surface normal due to the asymmetry of the interface. Nevertheless, the corrugation of the individual NiO and IrO₂ surfaces seems negligible. The corresponding E_{ad} is calculated to be 1.34 J m⁻², which is much higher than the adhesion strength of Pt/NiO interfaces. Considering these high E_{ad} and moderate lattice mismatch, we believe that the insertion of IrO₂ can energetically stabilize the Pt/NiO films.

4. Conclusions

To conclude, our DFT + U calculations demonstrate that the Pt/NiO interfaces have a weak stability from the energetic point of view. The fine interfacial microstructure may be destroyed during the practical application due to the rather weak strength of adhesion. The insertion of IrO₂ layers can enhance the

adhesion strength at the interfaces by a factor of 2–4. Although the large lattice mismatch at the Pt/IrO₂ interfaces induces a severe strain, it can be alleviated by rotating and translating the Pt slab appropriately. The enhanced interfacial bonding at the Pt/IrO₂ interface arises from the strong Pt–Ir metallic bonding as well as the Pt–O ionic bonding. In contrast, Pt/NiO interfacial adhesion is mainly determined by the Pt–O ionic bonding.

Acknowledgments

We gratefully acknowledge the financial support from the National Key Basic Research Program of China and the Natural Science Foundation of Zhejiang Province.

References

- [1] Seo S et al 2005 *Appl. Phys. Lett.* **87** 3
- [2] Jung R et al 2007 *Appl. Phys. Lett.* **91** 3
- [3] Park C, Jeon S H, Chae S C, Han S, Park B H, Seo S and Kim D W 2008 *Appl. Phys. Lett.* **93** 3
- [4] Yoshida C, Kinoshita K, Yamasaki T and Sugiyama Y 2008 *Appl. Phys. Lett.* **93** 3
- [5] Phark S H, Jung R, Chang Y J, Noh T W and Kim D W 2009 *Appl. Phys. Lett.* **94** 3
- [6] Kim D C et al 2006 *Appl. Phys. Lett.* **88** 3
- [7] Kawai M, Ito K and Shimakawa Y 2009 *Appl. Phys. Lett.* **95** 012109
- [8] Grogger W, Hofer F, Kraus B, Rom I, Sitte W and Warbichler P 2000 *Mikrochim. Acta* **133** 125
- [9] Venkataraman S, Kohlstedt D L and Gerberich W W 1992 *J. Mater. Res.* **7** 1126
- [10] Lu F H, Newhouse M L and Dieckmann R 1995 *J. Phys. Chem. Solids* **56** 715
- [11] Venkataraman S, Kohlstedt D L and Gerberich W W 1996 *J. Mater. Res.* **11** 3133
- [12] Shieu F S and Sass S L 1990 *Acta Metall. Mater.* **38** 1653
- [13] Kresse G and Furthmüller J 1996 *Phys. Rev. B* **54** 11169
- [14] Kresse G and Joubert D 1999 *Phys. Rev. B* **59** 1758
- [15] Blochl P E 1994 *Phys. Rev. B* **50** 17953
- [16] Bengone O, Alouani M, Blochl P and Hugel J 2000 *Phys. Rev. B* **62** 16392
- [17] Yu N, Zhang W B, Wang N, Wang Y F and Tang B Y 2008 *J. Phys. Chem. C* **112** 452
- [18] Bellini V, Di Giustino L and Manghi F 2007 *Phys. Rev. B* **76** 214432
- [19] Rohrbach A, Hafner J and Kresse G 2004 *Phys. Rev. B* **69** 075413
- [20] Shen Z X et al 1991 *Phys. Rev. B* **44** 3604
- [21] Lee P S, Pey K L, Mangelinck D, Ding J and Chan L 2003 *Solid State Commun.* **128** 325
- [22] Dudiy S, Hartford J and Lundqvist B I 2000 *Phys. Rev. Lett.* **85** 1898
- [23] Bader R F W 1990 *Atoms in Molecules: a Quantum Theory* (New York: Oxford University Press)
- [24] Yim W L and Kluner T 2008 *J. Comput. Chem.* **29** 1306
- [25] Johnson D F and Carter E A 2009 *J. Phys. Chem. A* **113** 4367
- [26] Xu G G, Wu Q Y, Chen Z G, Huang Z G, Wu R Q and Feng Y P 2008 *Phys. Rev. B* **78** 115420